Soft Matter

PAPER

Cite this: *Soft Matter*, 2016, 12, 8359

# Controlling swelling/deswelling of stimuli-responsive hydrogel nanofilms in electric fields†

Gabriel S. Longo,*[a] Monica Olvera de la Cruz[bc] and Igal Szleifer[cde]

Received 20th May 2016,
Accepted 12th September 2016

DOI: 10.1039/c6sm01172a

www.rsc.org/softmatter

The swelling/deswelling transition of pH-sensitive, electrode-grafted, hydrogel nanofilms when exposed to electric fields is studied by theoretical analysis. In acidic conditions, the response of these films to changes in pH is dominated by network–surface interactions, while intra-network electrostatic repulsions, which are highly modulated by the adsorption of salt ions, determine material response at a higher pH. Film thickness is a non-monotonic function of solution pH and displays a local maximum, a local minimum or both, depending on the salt concentration and the applied voltage. We suggest the use of these materials in the development of biosensors and control of enzyme activity.

## 1 Introduction

Stimuli-sensitive polymer hydrogels change their physical and chemical properties in response to moderate external perturbations. For example, ionic gels undergo many-fold volume changes upon varying solution pH[1–4] or salt concentration,[5–7] and polyelectrolyte (PE) gels shrink in the presence of modest electric fields.[8–10] These materials can be straightforwardly designed to be biocompatible as well as modified to incorporate functional groups or ligands to favor adsorption of bioactive molecules, which makes these hydrogels very attractive for biomedical applications.[11] In particular, based on the changes in pH that occur in the gastrointestinal tract, pH-responsive hydrogels are actively investigated as functional vehicles in the oral administration of small-molecule drugs[12–14] and therapeutic proteins.[15–21]

Thin hydrogel films are specially suitable for applications requiring fast response.[22] When one of the hydrogel's dimensions is sub-micrometric, swelling in response to changes in the environment occurs within the second timescale.[23] Application of thin hydrogel films include biosensors,[24,25] responsive supports for cell-culture,[26] drug/protein release devices[27] as well as materials for energy conversion.[28] In particular, there are many examples of the use of pH to trigger or control the response polymer films, such as adjusting the thickness of adsorbed weak polyelectrolyte layers,[29] changing the swelling temperature of grafted copolymer layers,[30] controlling cell adhesion on responsive polymer coatings,[31] and shifting the adsorption spectra of polymer-modified plasmonic surfaces.[32]

In this work, we provide theoretical predictions for the swelling/deswelling of pH-sensitive hydrogel nanofilms grafted onto an electrode when exposed to applied voltages. Our results show that depending on the applied potential and salt concentration, the thickness of the film is a non-monotonic function of the solution pH. As pH is varied, these nanofilms undergo transitions between regions of swelling and regions of deswelling.

When no external electric field is applied, pH-sensitive films swell as the solution pH (pH) increases above the intrinsic p$K_a$ of the network acidic units (p$K_a$). Swelling occurs due to electrostatic repulsions between increasing numbers of dissociated (charged) polymer segments. The acid–base equilibrium favors the dissociated species when pH > p$K_a$. The amount of charge on the polymer, however, does not completely define these intra-network repulsions; rather they are highly modulated by the adsorption of salt ions inside the material.

When the film is placed in contact with a low salt solution, confining ions inside the network is entropically costly. Only enough counterions adsorb to balance the network charge and neutralize the film. Intra-network repulsions extend for several nanometers and the film response to an increasing pH is two-fold. To reduce electrostatic repulsions, the amount of charge established on the network is much less than what the acid–base equilibrium favors. Namely, the network degree of dissociation is significantly lower than that of acid groups in a dilute (ideal) solution under the same conditions. In addition, because intra-network repulsions are relatively long-range, the

[a] *Instituto de Investigaciones Fisicoquímicas Teóricas y Aplicadas (INIFTA), CONICET, La Plata, Argentina. E-mail: longogs@inifta.unlp.edu.ar*
[b] *Department of Materials Science and Engineering, Northwestern University, Evanston, Illinois, USA*
[c] *Chemistry of Life Processes Institute, Northwestern University, Evanston, Illinois, USA*
[d] *Department of Biomedical Engineering, Northwestern University, Evanston, Illinois, USA*
[e] *Department of Chemistry, Northwestern University, Evanston, Illinois, USA*

† Electronic supplementary information (ESI) available: Details of the theoretical method and additional supporting results. See DOI: 10.1039/c6sm01172a

little charge established on the polymer network is sufficient to swell the film. Swelling occurs to place charged segments further apart thus reducing electrostatic repulsions.

Entropy loss of confining ions inside the film lowers as solution salt concentration increases. Both coions (negatively charged) and counterions (positively charged) adsorb, even if the network is weakly charged (low pH). These ions screen intra-network electrostatic repulsions, which become relatively short range and effectively extend for a few nanometers. When pH increases the film swells to reduce these repulsions, but there is little displacement from ideal dissociation.

An applied electric field induces charges on the electrode surface that supports the film. This charge modifies in a nontrivial manner the fine balance between intra-network repulsions, adsorption of salt ions, and acid–base equilibrium. Here, we report the non-monotonic swelling/deswelling with varying solution pH of grafted weak polyelectrolyte hydrogel nanofilms under external electric fields.

To study the swelling of hydrogel nanofilms, we use a theory that accounts for size, shape, conformation, and charge distribution of all molecular components. This theory can describe network charge regulation, because it predicts the state of dissociation of each acidic unit depending on position and local environment. This approach, based on work by Gong *et al.*[33] has been recently used to study pH-dependent swelling of poly(acrylic acid) (PAAc) hydrogel nanofilms under no external electric fields.[34] In the next section, we describe the most important features of this theoretical framework, while complete details of this molecular theory can be found in our previous work.[34]

## 2 Method

Consider a network of crosslinked weak polyelectrolyte chains (*e.g.*, PAAc) having some of its chains covalently grafted to a planar electrode. The Cartesian coordinate $z$ measures the distance from the grafting electrode placed at $z = 0$. This network is immersed in an aqueous salt solution that contains water molecules, protons, hydroxyl ions, and monovalent salt (NaCl) completely dissociated into sodium ($Na^+$) and chlorine ions ($Cl^-$). Far from the grafting electrode the system exchanges molecules with a bath (bulk) solution of controlled pH (pH) and salt concentration ($c_s$). An electric potential difference, $\Delta V$, is maintained between the electrode and the bulk solution.

The Helmholtz free energy of this system can be expressed as:

$$F = -TS_{nw} - TS_{tr} + U_{vdW} + U_{st} + F_{chm} + U_{el} \qquad (1)$$

where $T$ is the temperature of the bath solution, $S_{nw}$ is the entropy that results from the different molecular conformations of the network, $S_{tr}$ is the sum of the translational entropies of all free species, $U_{vdW}$ represents total attractive van der Waals energy, $U_{st}$ is the total repulsive steric (excluded volume) interaction, $F_{chm}$ is the chemical free energy that describes the acid–base equilibrium of ionizable network segments, and $U_{el}$ is the total electrostatic energy.

Each of terms in eqn (1) can be expressed as functional of one or more of the following functions: the distribution of probability of network conformations, the local density of each free species, the local degree of charge (or dissociation) of network units, and the local electrostatic potential. Optimization of the appropriate thermodynamic potential with respect to each of these functions leads to a series of integro-differential equations that can be numerically solved.

At each position, the equations to solve are the local incompressibility of the fluid and the Poisson equation. The unknowns in these equations are the position-dependent interaction potentials: the local osmotic pressure and the local electrostatic potential. Once these interaction potentials are calculated, all functions that compose the free energy are determined. Then, any thermodynamic quantity of interest can be derived from the free energy, while calculation of structural properties may require using the probability distribution of network conformations. The dependence of all functions that express the free energy on two interaction potentials makes clear the coupling existing between the physical interactions that contribute to the free energy and the chemical states of the different species.

An applied voltage fixes the value of the electrostatic potential at the surface of the metallic electrode. Namely, the boundary condition when solving the Poisson equation is

$$\Psi\ (z = 0) = \Delta V \qquad (2)$$

where $\Psi(z)$ is the position-dependent electrostatic potential. The charge density induced on the grafting electrode, $\sigma_M$, can be obtained from

$$\sigma_M = \varepsilon_w \left.\frac{d\Psi(z)}{dz}\right|_{z=0} \qquad (3)$$

where $\varepsilon_w$ is the absolute permittivity of water. In this work, we compare our results to the behavior of the same hydrogel nanofilms when grafted to a dielectric surface under no external electric field (hereinafter, we denote this last system as reference film).[34] In this last situation, the density of charge at the dielectric surface must be zero.[34] Namely, the boundary condition for the Poisson equation is $\sigma_M \equiv 0$. Note that subscript M refers to metal, since $\sigma_M$ is the charge density induced on the metallic electrode. For the sake of clarity, we have also used this notation when the boundary conditions are zero surface charge. We make the assumption that no chemical reactions occur at the electrode surface, which is a reasonable approximation for some metallic electrodes (gold or platinum). We have also assumed that the system is homogeneous in the $x$–$y$ plane.

Evaluation of the present theory requires defining a molecular model for the polymer network, which is schematically illustrated in Fig. 1. The network consists of 25-segment long chains interconnected at six-coordinated cross-linker units. Each segment bears an acidic group. Some chains are end-grafted to the electrode. Grafting points arrange on the electrode surface forming a square lattice with density 0.01 $nm^{-2}$. The polymer volume fraction of the hydrogel is 0.005, when the network is in the protonated state (low pH). A representative

 

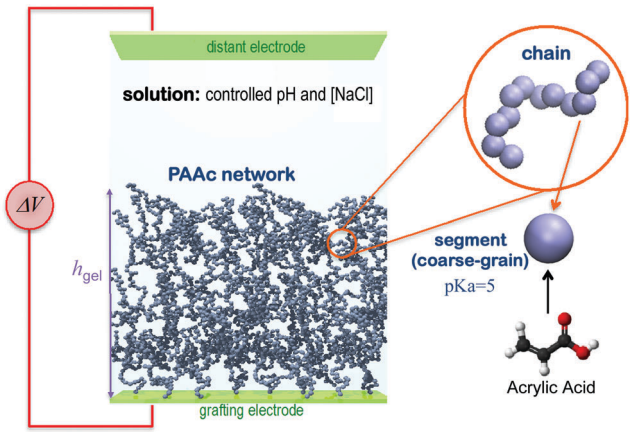


Fig. 1 Scheme representing the system of study. Crosslinked poly(acrylic acid) chains form the hydrogel backbone. The polymer network is grafted to a planar electrode. A voltage $\Delta V$ is applied between the grafting electrode and the bulk solution, which contains water and salt ions.

set of conformations of this polymer network is obtained performing molecular dynamics simulations. The intrinsic (logarithmic) acid–base equilibrium constant of network units is $pK_a = 5$, which represents a carboxylic acid such as acrylic acid. Then, the material that we model can represent a PAAc hydrogel chemically grafted to a planar gold electrode.

The independent variables of a calculation consist of pH and $c_s$, which define the bulk densities of all free species, and the applied voltage, $\Delta V$, which sets the boundary condition of the Poisson equation at the metallic surface of the grafting electrode. Other required input quantities are the volume and charge of all molecular components. More information of the method is provided in the ESI,† while a complete description of the molecular modeling of the polymer network, including details of the molecular dynamics simulations used to obtain conformations, and the numerical methodology employed to solve the theory equations can be found in our recent work.[34]

## 3 Results and discussion

We begin presenting results by describing the environment-sensitive swelling of these hydrogel nanofilms under applied electric fields. Because the polymer backbone is covalently grafted to the supporting electrode, the film can only modify its thickness, $h_{gel}$, in response to external stimuli. Film thickness can be calculated using:

$$h_{gel} = \frac{\int_0^\infty 2z\left\langle \phi_p(z)\right\rangle dz}{\int_0^\infty \left\langle \phi_p(z)\right\rangle dz} \quad (4)$$

where $\langle\phi_p(z)\rangle$ is the local volume fraction of polymer at a distance $z$ from the electrode. In our method, this local polymer volume fraction results from the minimization of the system free energy. Thus, a different polymer volume fraction profile is obtained for each set of experimental conditions, which introduces the dependence of film thickness on pH, $c_s$ and $\Delta V$. Similarly, we can obtain

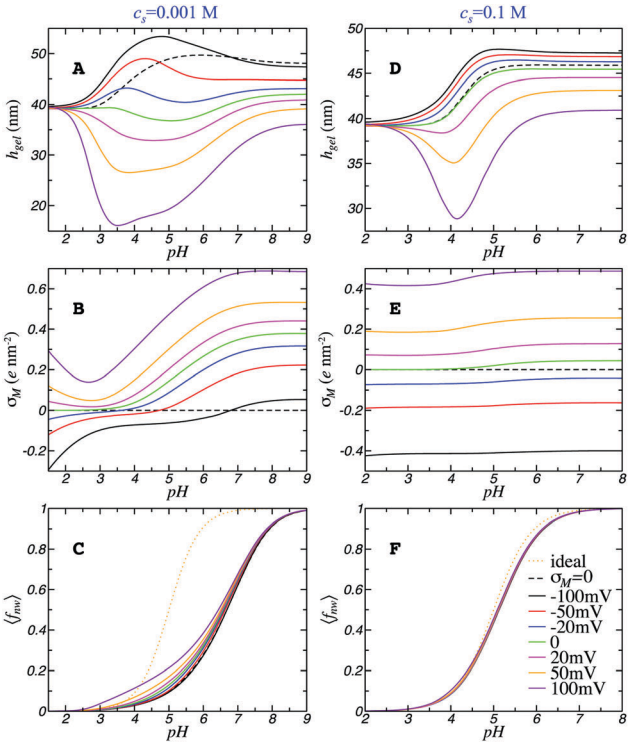


Fig. 2 Plot of film response as a function of pH for low (left-hand side panels) and high (right-hand side panels) salt concentration solutions. Film thickness (panels A and D), charge density induced on the electrode surface (B and E), and network degree of dissociation (C and F), are all shown for different applied voltages (solid lines) and $\sigma_M \equiv 0$ boundary conditions (dashed black lines). Ideal dissociation is displayed using a dotted orange line.

the local densities of all other molecular species as well as the local degree of dissociation of acidic units of the network.

Fig. 2 shows film thickness as a function of pH for different applied voltages and low (Fig. 2A) and high (Fig. 2D) salt concentration. Independently of solution composition, the film deswells ($h_{gel}$ decreases) as the applied voltage increases. This is because the resulting surface charge density on the metallic electrode, $\sigma_M$, increases with $\Delta V$ (Fig. 2B and E). Depending on the sign of $\sigma_M$, increasing the voltage leads to either weaker electrostatic repulsions or stronger attractions between the surface and the negatively charged polymer network. Several experimental results have shown that polyelectrolyte gels contract with increasing voltage when in contact with the electrode.[8,35–38] Yamamoto and Pincus[39] predicted that grafted strong PE brushes shrink with increasing applied voltage, because the polymer structure collapses to bring its charges closer to the surface and neutralize those induced on the grafting electrode. We will show that the same phenomenon dominates the behavior of pH-responsive hydrogel nanofilms at low pH.

Fig. 2 shows that film thickness is a non-monotonic function of pH. Both regions of swelling and deswelling are observed with increasing pH. Two observations from panels A and D allow us to uncover the underlying mechanism behind the pH-triggered swelling–shrinking behavior. First, swelling

(deswelling) can occur at low pH where the network is weakly charged, and intra-network repulsions are not strong enough to swell the film. Indeed, when the imposed boundary conditions are zero surface charge ($\sigma_M \equiv 0$) instead of an applied potential, the film remains in its unswollen state within this pH range (dashed black lines). Second, swelling (deswelling) is more accentuated for low salt solutions. These two features indicate that network–surface electrostatic interactions are responsible for the behavior observed at low pH.

Next, we show that as pH increases, the film transitions from the regime dominated by network–surface interactions at low pH to one regulated by intra-network repulsions. As a result, film thickness as a function of pH can display a maximum, a minimum or both depending on the solution composition and applied voltage. In the network–surface regime swelling or deswelling depends on the sign of electric charge established on the surface. At higher pH, the adsorption of ions modulates intra-network repulsions determining whether the film swells or compresses. This last phenomenon is also observed when film is grafted to an uncharged dielectric surface ($\sigma_M \equiv 0$) under similar conditions.

In Fig. 2B and E, we present the electric charge density induced on the grafting electrode $\sigma_M$ as a function of solution pH. To understand the non-monotonic dependence of film thickness on pH, let us first concentrate on the higher salt concentration shown in Fig. 2 ($c_s$ = 0.1 M). For these solutions, the electric charge on the grafting electrode does not significantly vary with pH, except when $\Delta V$ = 0, where the surface transitions from neutral to slightly positively charged as pH increases. The surface is negatively charged when $\Delta V > 0$ and positively charged otherwise.

Panels D and E of Fig. 2 show that regardless of bulk solution composition, film thickness increases if $\sigma_M < 0$ and decreases if $\sigma_M > 0$ with respect to the situation where the boundary condition is $\sigma_M \equiv 0$ (reference film). This result is consistent with the predictions of Drozdov *et al.*,[40] within the framework of continuum modeling, which indicate that a positive area density of charge at the supporting surface of a poly(acrylamide-co-acrylic acid) nanogel layer leads to swelling, while a negative surface charge decreases the degree of swelling. Our results show that applied $\Delta V$ and $\sigma_M$, obtained through eqn (3), have the same sign at high salt concentration (Fig. 2E). Thus, under such conditions the film swells if a negative potential is applied and shrinks if the applied potential is negative, relative to the reference film. This last statement, however, is not necessarily true at low salt concentration (see Fig. 2A and B).

In Fig. 2C and F we plot network degree of dissociation, calculated using:

$$\langle f_{nw} \rangle = \frac{\int_0^\infty f_{nw}(z) \left\langle \phi_p(z) \right\rangle dz}{\int_0^\infty \left\langle \phi_p(z) \right\rangle dz} \quad (5)$$

where $f_{nw}(z)$ is the local degree of dissociation at distance $z$ from the grafting electrode. For high salt solutions, the network state of dissociation given $\Delta V$ is roughly the same as that resulting from zero surface charge. The adsorption of ions inside the film is also similar (see ESI†). Then, film swelling under zero surface charge provides a reference of the intra-network repulsions that drive swelling above p$K_a$. Indeed, independently of the applied potential, the film swells in the same pH intervals where the reference film does (Fig. 2D).

If surface charge is positive at low pH ($\Delta V > 0$ for $c_s$ = 0.1 M), the film deswells with increasing pH (see Fig. 2D and E). Under these conditions, intra-network repulsions are not strong enough to swell the film. Through deswelling, the network can place its negatively charged units closer to the surface, without the cost of large intra-network repulsions. When the surface charge is negative ($\Delta V < 0$ for $c_s$ = 0.1 M), additional swelling with respect to the reference film occurs to place charged units further apart from the like-charged surface.

At low salt concentration, electrostatic interactions are effectively longer range than in high salt environments. As a consequence, swelling behavior displays more complex features (see Fig. 2A). Qualitatively, swelling (deswelling) can be understood in terms of the same competing interactions that describe the behavior at high salt conditions, but the adsorption of salt ions plays a critical role. At low pH, where intra-network repulsions are weak, surface charge can drive swelling or deswelling of the film depending on the sign of the electric charge established on the surface. Compared to reference conditions, the film is thicker if $\sigma_M < 0$ and thinner if $\sigma_M > 0$ (compare Fig. 2A and B). Interestingly, to favor attractions with the positively charged surface for high voltages (and low pH), the network dissociates more than ideally (see Fig. 2C).

When $\Delta V > 0$, the behavior observed in panels A and B of Fig. 2 is relatively similar to what occurs at higher salt concentration. When pH increases from a low value, the film first shrinks due to positive charges on the grafting electrode, but then swells due to increasing intra-network repulsions as acid groups dissociate (see Fig. 2C). Compared to high salt conditions, swelling and deswelling span wider pH intervals.

An interesting response is observed for the most negative voltages (Fig. 2A and B). At low pH, the film swells first due to the like-sign surface charge and then because of intra-network repulsions (the reference film swells). However, as pH increases, film thickness reaches a maximum, followed by shrinking at higher pH. Such deswelling occurs because of the rising ionic strength that results from the adsorption of salt ions as network dissociation proceeds. A higher ionic strength results in stronger screening of intra-network repulsions, which become effectively shorter-range, thus allowing the observed deswelling. Indeed, ionic strength inside the film increases 15–30 fold, depending on $\Delta V$, as pH increases in this deswelling region (see ESI†). In comparison, such change is less than 1.2 when $c_s$ = 0.1 M. Deswelling due to salt-driven screening of intra-network repulsions has also been predicted for zero surface charge.[34] Interestingly, the sign of electrode charge reverses within this deswelling region and network–surface interactions become attractive (see Fig. 2A and B), which additionally favors film compression.

We close the description of swelling behavior at low $c_s$ by discussing two particular cases. When $\Delta V$ = −20 mV, the film

 

experiences both local maximum and minimum with increasing pH. The initial swelling–deswelling transition occurs because network–surface interactions change from repulsive to attractive, while the subsequent swelling is due to intra-network repulsions. When $\Delta V = 0$, film thickness is relatively similar within the whole pH range. The magnitude of the response is much less significant than that of the reference film. This behavior is completely different from what occurs at high salt concentration, where swelling at $\Delta V = 0$ and that at $\sigma_M \equiv 0$ are roughly identical.

Fig. 3 shows total cumulative charge, $q_{tot}$, as a function of the distance from the grafting electrode as well as individual contributions from each ionic species. Two different sets of conditions are presented in Fig. 3 that correspond to the minimum thickness (panel A) and maximum swelling (panel B) predicted in Fig. 2D for high $c_s$. Under no external electric field, the film satisfies local electroneutrality.[34] Namely, at any distance $z$ from the dielectric supporting surface, the total cumulative charge satisfies $q_{tot}(z) \approx 0$, this condition results from a local balance between physical interactions and chemical states. The only constraint that we impose in our calculations is global electroneutrality. Namely, total cumulative charge must be zero when considering the fluid system from immediately above the surface up to bulk solution $\lim_{z\to\infty} q_{tot}(z) = 0$. Local electroneutrality is not maintained when an external electric field is applied, as seen both panels of Fig. 3. However, displacements from local charge-neutrality occur only in the very few nanometers closest to the grafting electrode (typically less than 5 nm as illustrated in Fig. 3). Further apart from the surface, local electroneutrality is achieved in all regions, inside the film, in the solution and in the film–solution interface, independently of the applied potential and the solution composition.

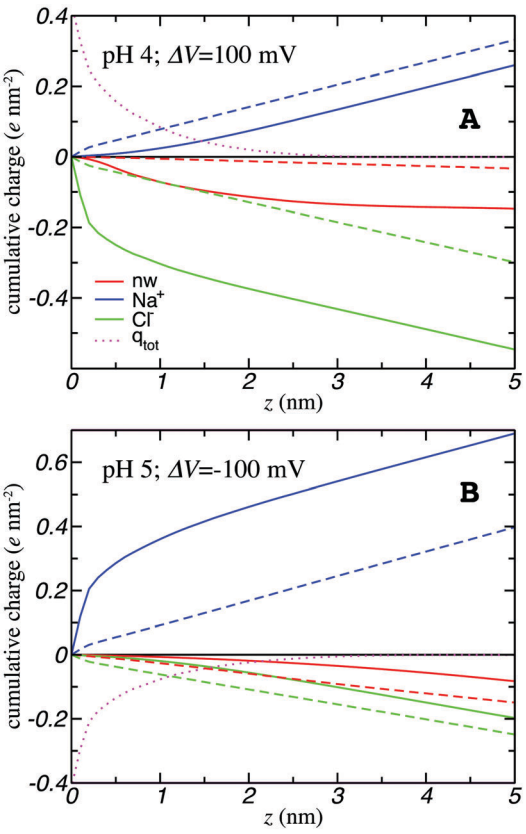


Fig. 3 Plot of total cumulative charge per unit area (magenta dotted line) and individual contributions from different ionic species (solid lines), including the polymer network (red line), as a function of the distance from the grafting electrode. Dashed lines show species cumulative charge when $\sigma_M \equiv 0$. At the surface, the total cumulative charge equals the density of charge induced on the electrode, $q_{tot}(z = 0) = \sigma_M$. Experimental conditions correspond to those of minimum and maximum thickness predicted in Fig. 2D, respectively. Salt concentration is 0.1 M.

The conditions leading to minimum and maximum thickness in Fig. 2D illustrate hydrogel response in the low-pH regime, where surface–network interactions drive swelling or deswelling. Shrinking resulting in minimum thickness is associated with a high density of positive charge on the surface. To neutralize the electrode charge, more $Cl^-$ and less $Na^+$ ions are present in the region near the surface, with respect to the reference film (see Fig. 3A). Deswelling allows the network to bring significantly more charge to this region, as compared to uncharged dielectric surface, without paying the price of strong intra-network repulsions. The situation reverses under the conditions of maximum thickness, where the surface charge density is high and negative. Compared to the reference film, there are significantly more $Na^+$ near the electrode (see Fig. 3B), but the polymer brings less charge to this region. Intra-network repulsions under these conditions are strong enough to swell the film. Additional swelling with respect to the reference film occurs to place charged units further apart from the electrode. We remind the reader that given the pH at this relatively high salt concentration, the average degree of charge of network units is roughly identical whether an electric potential is applied or not (see Fig. 2F).

Inside the film, pH drops with respect to the bulk solution. This occurs because of the constraint that the dissociation of confined acid units and the resulting electrostatic repulsions impose on the local density of protons. To describe this behavior, we define the local pH as:

$$\mathrm{pH}(z) = -\log_{10}[\mathrm{H}^+](z) \quad (6)$$

where $[H^+](z)$ is the local concentration of protons. The pH established inside the film can be adequately described using the average of the local pH over the film thickness,

$$\mathrm{pH}_{gel} = \frac{1}{h_{gel}}\int_{z_0}^{h_{gel}} \mathrm{pH}(z) \quad (7)$$

where $z_0 = 5$ nm is introduced to exclude the region of non-local electroneutrality (close to the electrode; see Fig. 3) from the calculation of the gel pH. Then, the drop in pH inside the film is

$$\Delta\mathrm{pH} = \mathrm{pH}_{gel} - \mathrm{pH} \quad (8)$$

The magnitude of such drop in pH depends on the solution composition and the density of network ionizable groups,[34] as can be seen in Fig. 4. Applying an electric potential does not significantly affect the pH established inside the film, which results similar to that when $\sigma_M \equiv 0$ (see Fig. 4). Thus, Fig. 4 suggests that $\mathrm{pH}_{gel}(\Delta V) \approx \mathrm{pH}_{gel}(\sigma_M \equiv 0)$ is a reasonable

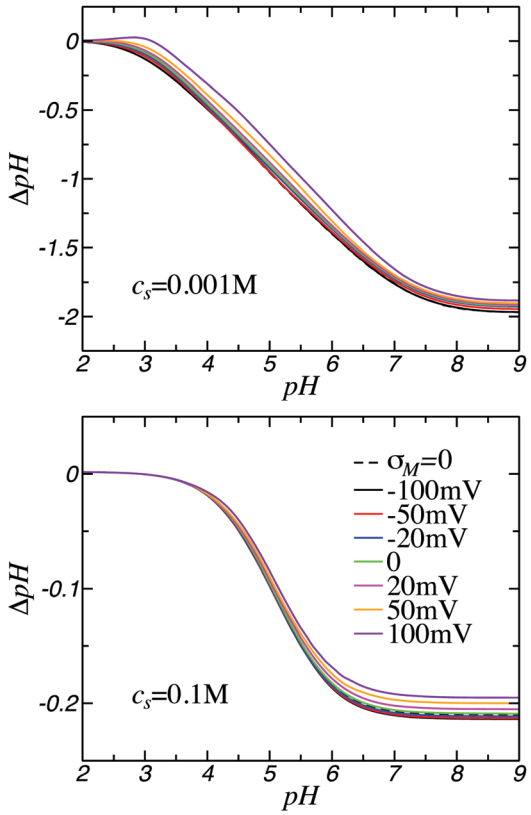


Fig. 4 Plot of the drop in pH inside the film $\Delta pH = pH_{gel} - pH$ as a function of solution pH for different applied voltages and low (top panel) and high (bottom panel) salt concentration. In both panels, a black dashed line represents the drop in pH when no external electric field is applied ($\sigma_M \equiv 0$).

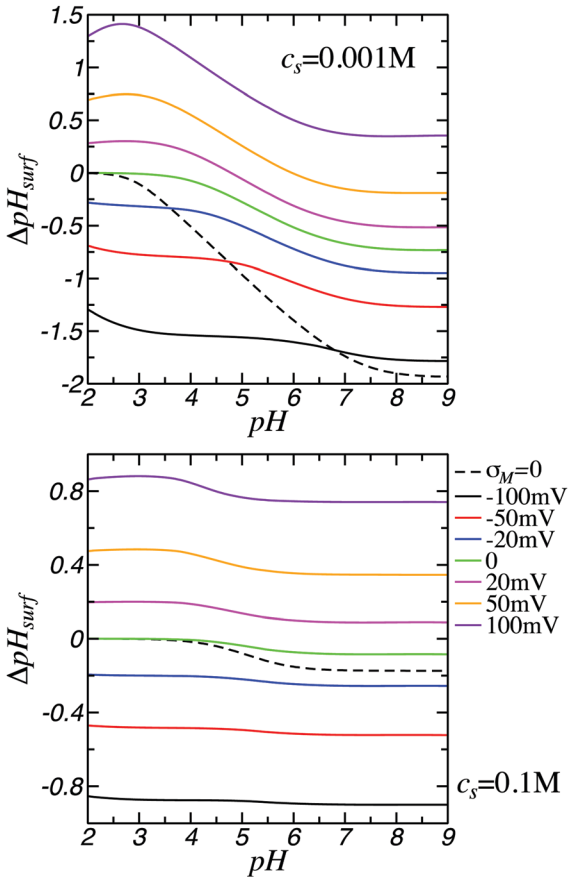


Fig. 5 Plot of excess surface pH (with respect to the bulk solution) $\Delta pH_{surf} = pH(z = 0) - pH$ as a function of solution pH. Upper and lower panels correspond to low and high salt concentrations respectively. In both panels, a black dashed line gives $\Delta pH_{surf}$ for $\sigma_M \equiv 0$ boundary conditions.

approximation in for the whole range of experimental conditions considered. The absolute error of using this approximation is less than 0.2 units (of pH) when $c_s$ = 0.001 M and less than 0.015 units when $c_s$ = 0.1 M. Indeed, local pH is not very sensitive to the applied voltage, except in the region nearest the grafting surface (see ESI†).

However, in the few nanometers closest to the surface the situation is completely different. Local pH strongly depends on the applied voltage (see ESI†). In particular, immediately above the electrode, pH can be regulated using the applied voltage without altering $pH_{gel}$. To illustrate how surface pH can be controlled, Fig. 5 shows

$$\Delta pH_{surf} = pH(z = 0) - pH \quad (9)$$

where $pH(z = 0)$ is the local pH immediately above the grafting electrode. Note that for the uncharged dielectric grafting surface, $pH(z = 0)$ and $pH_{gel}$ must be similar, within the local fluctuation occurring inside the film. Namely, surface pH and gel pH are similar for this boundary condition. Thus, $\Delta pH_{surf}$ for $\sigma_M \equiv 0$ gives additional information on ΔpH (for both boundary conditions according to the results of Fig. 4). Note that in Fig. 5 curves for different applied potentials are roughly parallel to each other. This behavior results because to a first order approximation $\Delta pH_{surf}(pH)$ is proportional to $\Delta V$ (see ESI†).

The results presented in Fig. 5 are consistent with experimental findings that report a lower pH in the vicinity of the anode for positive applied electric potentials.[36,41,42] Together Fig. 4 and 5 show that applying an electric potential allows controlling the pH near the electrode without altering the environment in other regions of the hydrogel; this environment can be independently modified varying the solution pH and salt concentration.

## 4 Conclusions

The ability to control film thickness by means of an applied voltage has technological relevance in the development of biomolecular sensors. We have recently shown that the presence of peptides[43] and proteins[44] modifies the swelling behavior of the pH-sensitive nanofilms under no external electric field. In this work, using a molecular theory, we predict that the thickness of pH-responsive hydrogel nanofilms can be externally controlled using the solution composition and an electric field. Depending on the applied voltage, hydrogel nanofilms display swelling–deswelling transitions upon changes in pH. As the solution pH increases these transitions are associated with the crossing from a

regime where network–surface electrostatic interactions dominate swelling behavior to one where the intra-network repulsions prevail. The adsorption of salt ions plays a fundamental role in modulating these interactions in both regimes. For example, varying the solution pH at low salt concentration can induce surface charge reversal (at constant applied voltage), thus film-surface interactions change from repulsive to attractive.

Varying the applied potential and the solution composition enables controlling the chemical environment in different regions of the material. Except in the region nearest the grafting surface, local pH inside the film is controlled by the solution composition (and the polymer volume fraction) regardless of the applied voltage. However, immediately above the electrode, surface pH can be regulated using the applied potential. Local pH is an important quantity, which defines the protonation state of adsorbed peptides and proteins.[43,44] We envision a hydrogel film whose gel pH is (indirectly) controlled to drive adsorption of enzymes inside the material from a dilute solution, while the applied voltage is set to regulate the activity of these molecules near the surface. At finite concentrations, however, the presence of the adsorbate modifies the gel pH.[45]

## Acknowledgements

G. S. L. acknowledges supports from ANPCyT (FonCyT, PICT-2014-3377), Argentina. M. O. C. thanks support from the Center for Bio-Inspired Energy Science (CBES), which is an Energy Frontier Research Center funded by the U.S. Department of Energy, Office of Science, Office of Basic Energy Sciences, under Award Number DE-SC0000989. I. S. thanks a grant from the NSF, CBET-1264696.

## References

1 T. Tanaka, D. Fillmore, S.-T. Sun, I. Nishio, G. Swislow and A. Shah, *Phys. Rev. Lett.*, 1980, **45**(20), 1636–1639.
2 T. G. Park and A. S. Hoffman, *J. Appl. Polym. Sci.*, 1992, **46**(4), 659–671.
3 O. E. Philippova, D. Hourdet, R. Audebert and A. R. Khokhlov, *Macromolecules*, 1997, **30**(26), 8278–8285.
4 P. F. Kiser, G. Wilson and D. Needham, *Nature*, 1998, **394**(6692), 459–462.
5 I. Ohmine and T. Tanaka, *J. Chem. Phys.*, 1982, **77**(11), 5725–5729.
6 C. H. Jeon, E. E. Makhaeva and A. R. Khokhlov, *Macromol. Chem. Phys.*, 1998, **199**(12), 2665–2670.
7 B. Zhao and J. S. Moore, *Langmuir*, 2001, **17**(16), 4758–4763.
8 T. Tanaka, I. Nishio, S.-T. Sun and S. Ueno-Nishio, *Science*, 1982, **218**(4571), 467–469.
9 I. C. Kwon, Y. H. Bae and S. W. Kim, *Nature*, 1991, **354**(6351), 291–293.
10 Y. Osada, H. Okuzaki and H. Hori, *Nature*, 1992, **355**(6357), 242–244.
11 J. Kopeček, *Biomaterials*, 2007, **28**(34), 5185–5192.
12 G. M. Eichenbaum, P. F. Kiser, D. Shah, S. A. Simon and D. Needham, *Macromolecules*, 1999, **32**(26), 8996–9006.
13 W.-Q. Liu, Y.-Y. Liu, X.-Q. Liao and W. Tian, *Mater. Sci. Eng., C*, 2012, **32**(4), 953–960.
14 R. Jayakumar, A. Nair, N. S. Rejinold, S. Maya and S. V. Nair, *Carbohydr. Polym.*, 2012, **87**(3), 2352–2356.
15 M. Torres-Lugo and N. A. Peppas, *Macromolecules*, 1999, **32**(20), 6646–6651.
16 B. Kim, K. La Flamme and N. A. Peppas, *J. Appl. Polym. Sci.*, 2003, **89**(6), 1606–1613.
17 K. Nakamura, R. J. Murray, J. I. Joseph, N. A. Peppas, M. Morishita and A. M. Lowman, *J. Controlled Release*, 2004, **95**(3), 589–599.
18 T. Yamagata, M. Morishita, N. J. Kavimandan, K. Nakamura, Y. Fukuoka, K. Takayama and N. A. Peppas, *J. Controlled Release*, 2006, **112**(3), 343–349.
19 D. A. Carr and N. A. Peppas, *J. Biomed. Mater. Res., Part A*, 2010, **92**(2), 504–512.
20 M. C. Koetting and N. A. Peppas, *Int. J. Pharm.*, 2014, **471**(1–2), 83–91.
21 D. Suhag, R. Bhatia, S. Das, A. Shakeel, A. Ghosh, A. Singh, O. P. Sinha, S. Chakrabarti and M. Mukherjee, *RSC Adv.*, 2015, **5**(66), 53963–53972.
22 I. Tokarev and S. Minko, *Soft Matter*, 2009, **5**(3), 511–524.
23 T. Tanaka and D. J. Fillmore, *J. Chem. Phys.*, 1979, **70**(3), 1214–1218.
24 X. Zhang, Y. Guan and Y. Zhang, *Biomacromolecules*, 2012, **13**(1), 92–97.
25 A. Mateescu, Y. Wang, J. Dostalek and U. Jonas, *Membranes*, 2012, **2**(1), 40–69.
26 Z. Zhao, J. Gu, Y. Zhao, Y. Guan, X. X. Zhu and Y. Zhang, *Biomacromolecules*, 2014, **15**(9), 3306–3312.
27 W. Zhu, L. Xiong, H. Wang, G. Zha, H. Du, X. Li and Z. Shen, *Polym. Chem.*, 2015, **6**(40), 7097–7099.
28 A. Erbas and M. Olvera de la Cruz, *ACS Macro Lett.*, 2015, **4**(8), 857–861.
29 S. S. Shiratori and M. F. Rubner, *Macromolecules*, 2000, **33**(11), 4213–4219.
30 M. Kaufmann, Y. Jia, L. Renner, S. Gupta, D. Kuckling, C. Werner and T. Pompe, *Soft Matter*, 2010, **6**(5), 937–944.
31 J. Gensel, T. Borke, N. P. Pérez, A. Fery, D. V. Andreeva, E. Betthausen, A. H. E. Müller, H. Möhwald and E. V. Skorb, *Adv. Mater.*, 2012, **24**(7), 985–989.
32 I. Tokareva, S. Minko, J. H. Fendler and E. Hutter, *J. Am. Chem. Soc.*, 2004, **126**(49), 15950–15951.
33 P. Gong, J. Genzer and I. Szleifer, *Phys. Rev. Lett.*, 2007, **98**(1), 018302.
34 G. S. Longo, M. Olvera de la Cruz and I. Szleifer, *J. Chem. Phys.*, 2014, **141**(12), 124909.
35 Y. Osada and M. Hasebe, *Chem. Lett.*, 1985, (9), 1285–1288.
36 S. H. Yuk, S. H. Cho and H. B. Lee, *Pharm. Res.*, 1992, **9**(7), 955–957.
37 T. Budtova, I. Suleimenov and S. Frenkel, *Polym. Gels Networks*, 1995, **3**(3), 387–393.
38 K. Seon Jeong, K. Han II, P. Sang Jun, K. In Young, L. Sang Hoon, L. Tae Soo and I. K. Sun, *Smart Mater. Struct.*, 2005, **14**(4), 511.

39 T. Yamamoto and P. A. Pincus, *Europhys. Lett.*, 2011, **95**(4), 48003.
40 A. D. Drozdov, C. G. Sanporean and J. deClaville Christiansen, *Mater. Today Commun.*, 2016, **6**, 92–101.
41 I. Kaetsu, K. Uchida, Y. Morita and M. Okubo, *Int. J. Radiat. Appl. Instrum., Part C*, 1992, **40**(2), 157–160.
42 S. Murdan, *J. Controlled Release*, 2003, **92**(1–2), 1–17.
43 G. S. Longo, M. Olvera de la Cruz and I. Szleifer, *Langmuir*, 2014, **30**(50), 15335–15344.
44 C. F. Narambuena, G. S. Longo and I. Szleifer, *Soft Matter*, 2015, **11**(33), 6669–6679.
45 G. S. Longo and I. Szleifer, *J. Phys. D: Appl. Phys.*, 2016, **49**(32), 323001.

 